Electronic Supplementary Material (ESI) for Nanoscale Advances.

Electrocatalytic Study for Hydrogen Evolution Reaction on MoS_2/BP and MoSSe/BP in Acidic Media†

Arunima Singh*, Manjari Jain, Preeti Bhumla, Saswata Bhattacharya*

Department of Physics, Indian Institute of Technology Delhi, New Delhi 110016, India

E-mail: saswata@physics.iitd.ac.in[SB],Arunima.Singh@physics.iitd.ac.in[AS]

Phone: +91-2659 1359. Fax: +91-2658 2037

Supporting Information

I. Structural, Electronic and Optical Properties of MoS_2/BP and MoSSe/BP
II. Planar Averaged Charge Density Plot of MoS_2/BP and MoSSe/BP
III. Planar Averaged Charge Density Plot of MoS_2/BP with 1 Solvated H^+
IV. Radial Distribution Function at 0K and 300K Temperatures for MoS_2/BP Configuration
V. Volmer step for $H_{adsorbed}$ on MoS_2/BP and MoSSe/BP vdW HTSs
VI. Heyrovsky reaction path for $H_{adsorbed}$ at P site on MoS_2/BP vdW HTSs

VII. Heyrovsky reaction path for $H_{adsorbed}$ at P site on MoS_2/BP vdW HTSs for 1/4 H^+ conc.
VIII. 3×3 MoS_2/BP Configurations
IX. 3×3 MoS_2/BP Configurations with H_{down} Water Layer Orientation
X. Electrode Potential of 2×2 MoS_2/BP and MoSSe/BP
XI. Electrode Potential of 4×4 MoS_2/BP and MoSSe/BP
XII. H_{down} Water Orientation Reaction Path and Electrode Potential
XIII. Tafel Reaction Steps for 2×2 MoS_2/BP in case of $4H_2O$

Structural, Electronic and Optical Properties of MoS_2/BP and MoSSe/BP

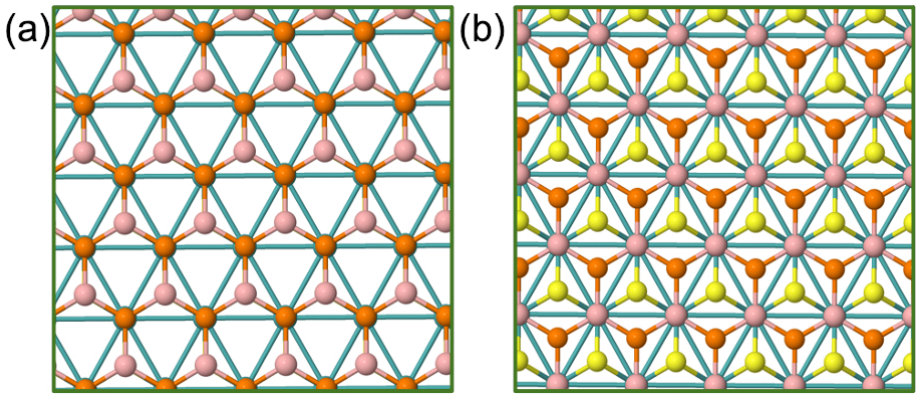

Fig. S1: (Color online) (a) and (b) are the two stacking styles of MoS_2/BP analyzed in our study. Configuration (b) has minimum binding energy.

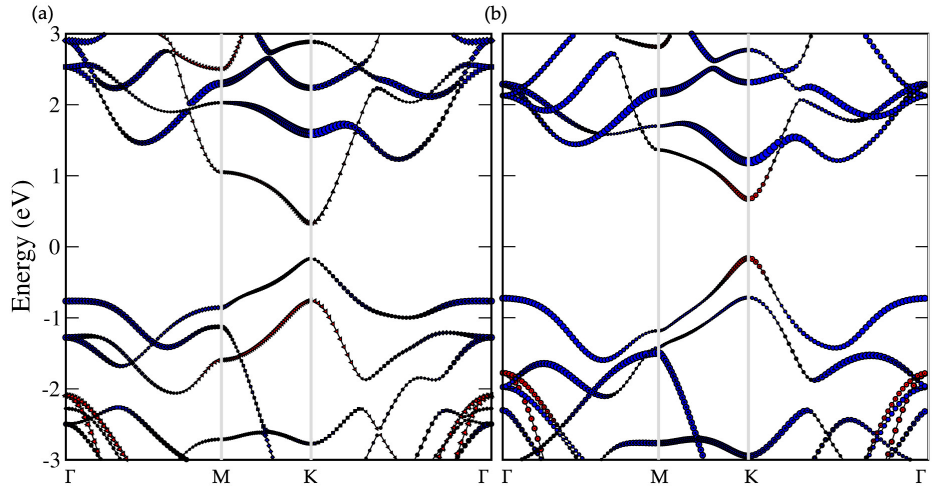

Fig. S2: (Color online) (a) Type II bandstructure obtained for MoSSe/BP vdW HTS; (b) Type I bandstructure obtained for MoS_2/BP vdW HTS. (xc functional: PBE)

In case of MoSSe/BP, BP contributes to the CBm (Conduction Band Minimum) and MoSSe contributes to the VBM (Valence Band Maximum). MoS_2/BP shows type 1 band edge alignment where MoS_2 straddles BP band edges.

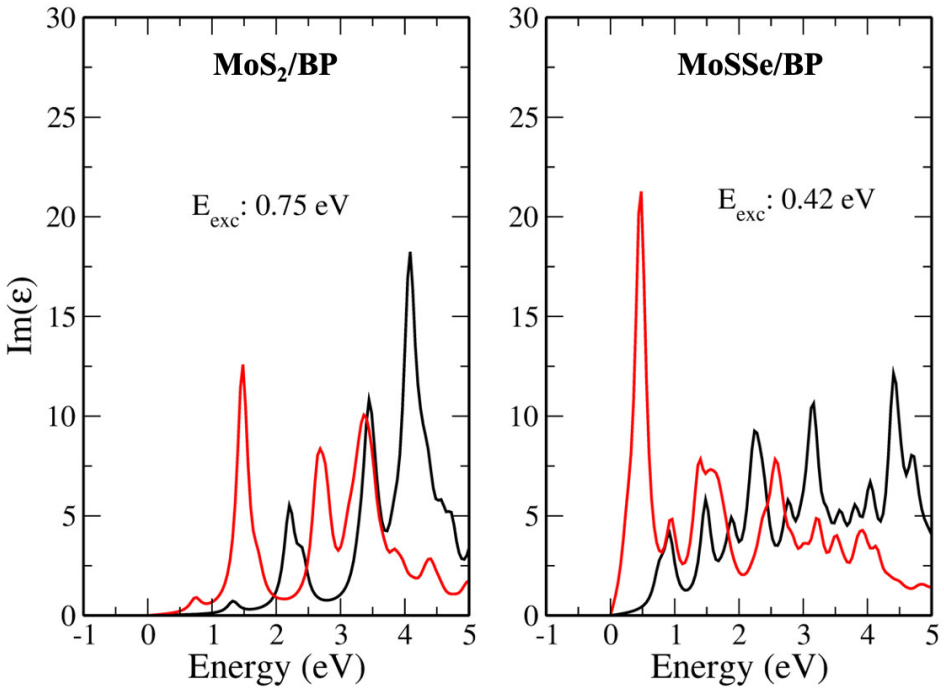

Fig. S3: (Color online) Exciton binding energy obtained for MoS_2/BP and MoSSe/BP vdW HTS.

The optical properties have also been calculated by the GW approach (Many Body Perturbation Theory (MBPT)). Fig. S3 shows the optical response using GW@BSE method that calculates the dielectric function. This is a complex function where the expression for interband process is the imaginary part thereby giving the absorption spectra. The real part (Re(ε)) is deduced from the Kramers-Kronig relation. We observe both the vdW HTSs (MoS_2/BP and MoSSe/BP) having response in the visible region. We have calculated the exciton binding energy (E_B) using the Bethe-Salpeter Equation. We observe small E_B that indicates its applicability in photoelectrochemical processes.

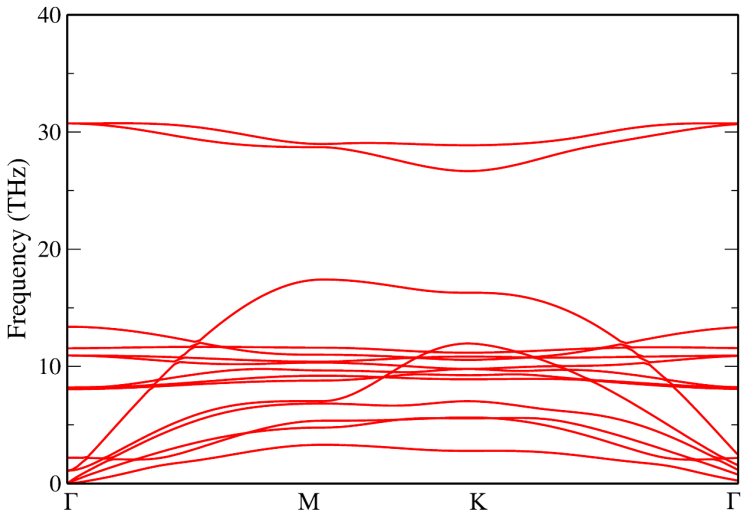

Fig. S4: (Color online) Phonon dispersion plot for MoS_2/BP .

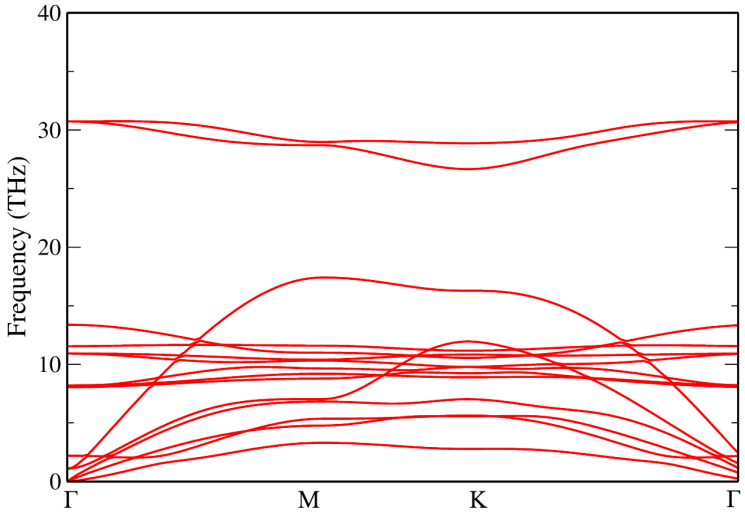

Fig. S5: (Color online) Phonon dispersion plot for MoSSe/BP .

We have obtained the binding energies per atom (BE) and work of adhesion (W_{ad}) for each bilayer model (MoS_2/BP and MoSSe/BP) with the supercells of 2×2, 3×3, 4×4, 5×5 and 6×6. The equation for work of adhesion is as follows:

$$W_{ad} = \frac{E_{BP} - E_{MoS_2} - E_{MoS_2/BP}}{2A}$$

The values are consistent with all the cases as observed in the following table.

Table S1: BE and W_{ad} for MoS_2/BP and MoSSe/BP with and without H^+ in water layer.

System	BE/W_{ad}				
	2×2	3×3	4×4	5×5	6×6
	eV	eV	eV	eV	eV
MoS_2/BP	-0.047/-0.014	-0.048/-0.014	-0.048/-0.015	-0.048/-0.016	-0.048/-0.016
MoSSe/BP	-0.050/-0.015	-0.051/-0.015	-0.051/-0.015	-0.051/-0.015	-0.051/-0.015

Planar Averaged Charge Density Plot of MoS_2/BP and MoSSe/BP

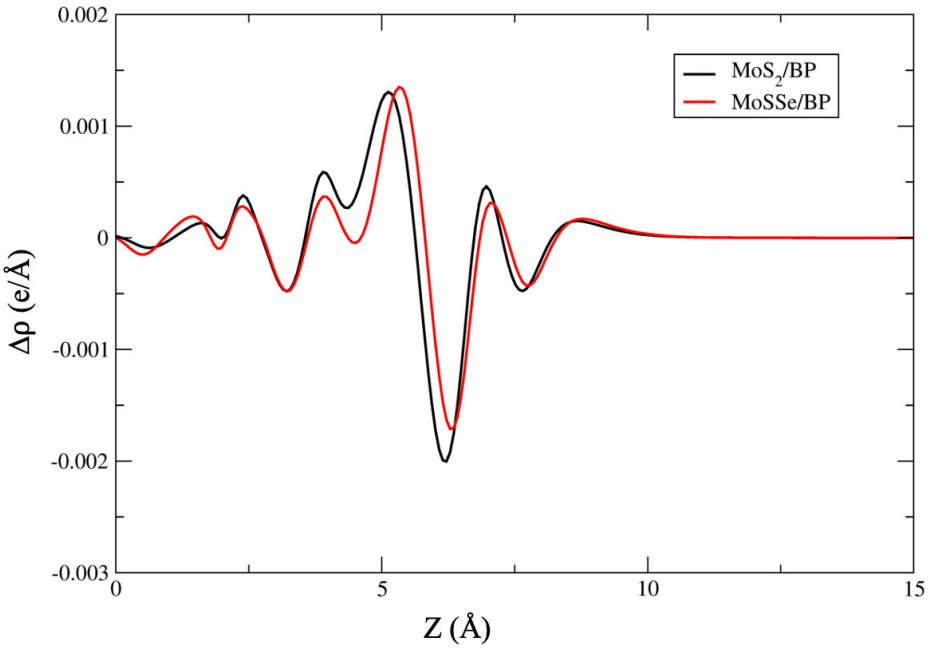

Fig. S6: (Color online) Planar averaged charge density plot for MoS_2/BP and MoSSe/BP vdW HTS.

The planar averaged charge density difference $\Delta\rho$ is calculated by:

$$\Delta\rho = \rho(\text{vdW HTSs}) - \rho(MoS_2 \text{ or MoSSe}) - \rho(\text{BP}) \quad (1)$$

where ρ(vdW HTSs), $\rho(MoS_2)$, ρ(MoSSe) and ρ(BP) are the charge densities of the vdW HTS, monolayer MoS_2, monolayer MoSSe and monolayer BP, respectively.

Planar Averaged Charge Density Plot of MoS_2/BP with 1 Solvated H^+

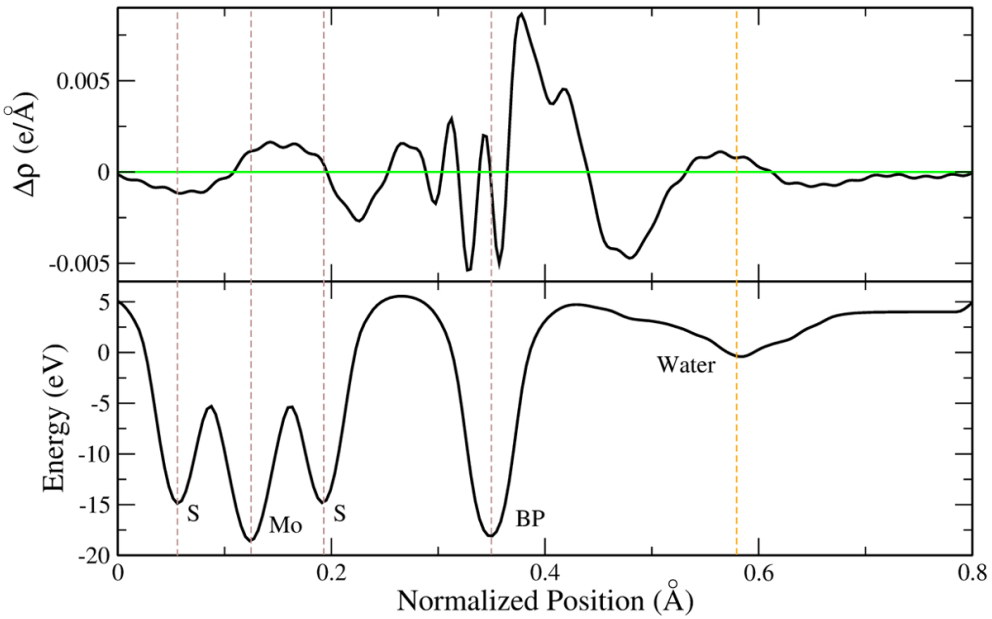

Fig. S7: (Color online) Planar averaged charge density and electrostatic potential plot for MoS_2/BP (with 1 H^+).

Fig. S7 shows the planar averaged charge density plot and the corresponding electrostatic potential plot for MoS_2/BP with 1 solvated H^+. The electrostatic potential plot explains the electrostatic potential corresponding to each atomic layer. We observe significant charge transfer at the BP and water interface.

Radial Distribution Function at 0K and 300K Temperatures for MoS_2/BP Configuration

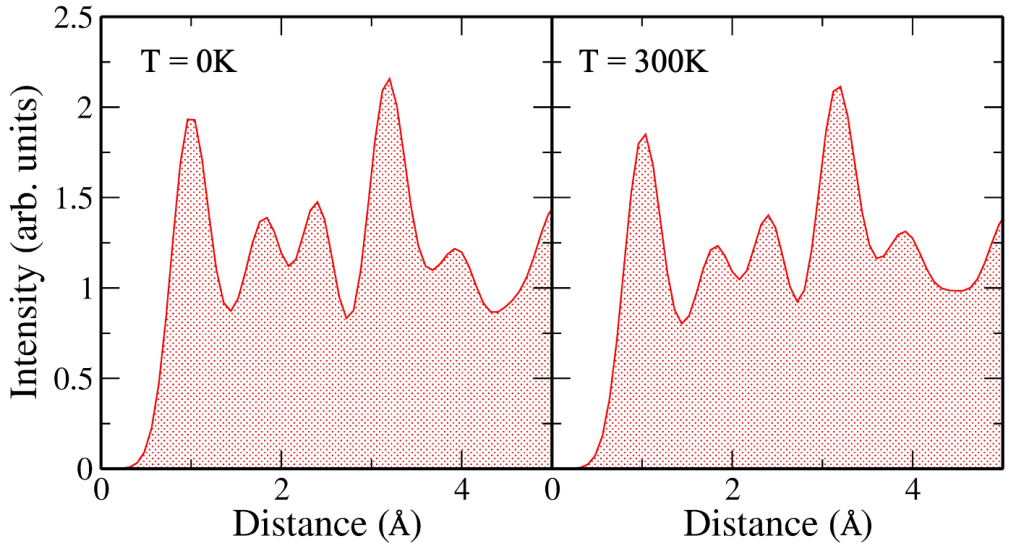

Fig. S8: (Color online) Radial distribution function of MoS_2/BP at two different temperatures T= 0K and T= 300K.

The radial distribution function here indicates the structural similarity of the MoS_2/BP with water layer at 0K and 300K. The water orientation thus obtained corroborates with the initial optimized configuration.

Volmer step for $H_{adsorbed}$ on MoS_2/BP and MoSSe/BP vdW HTSs

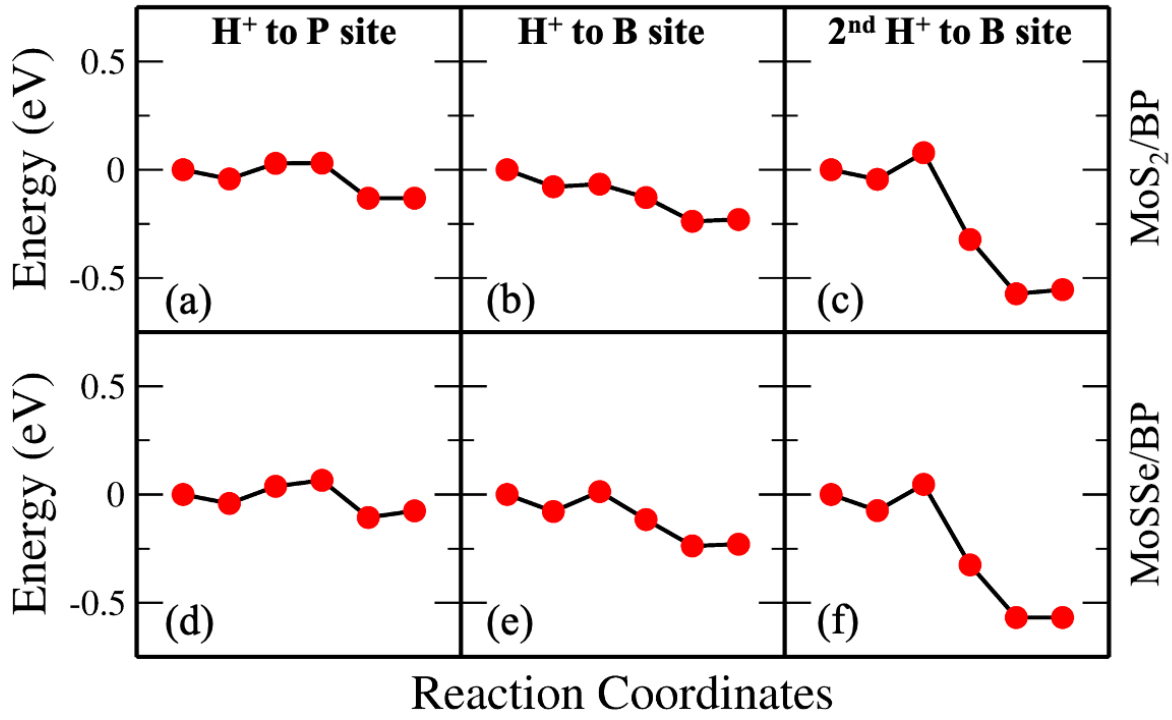

Fig. S9: (Color online) Volmer reaction path for $H_{adsorbed}$ at P site ((a) and (d)), B site ((b) and (e)) on MoS_2/BP and MoSSe/BP vdW HTSs. (c) and (f) H^+ adsorbed on P site along already H adsorbed on B site.

Heyrovsky reaction path for $H_{adsorbed}$ at P site on MoS_2/BP vdW HTSs

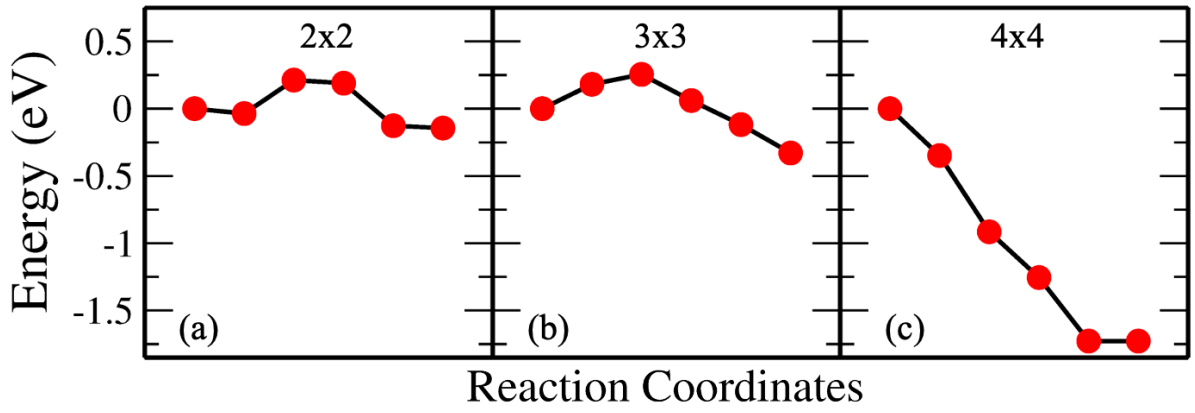

Fig. S10: (Color online) Heyrovsky reaction path for $H_{adsorbed}$ at P site on MoS_2/BP vdW HTSs for (a) 2×2, (b) 3×3 and(c) 4×4 supercell.

Heyrovsky reaction path for $H_{adsorbed}$ at P site on MoS_2/BP vdW HTSs for 1/4 H^+ conc.

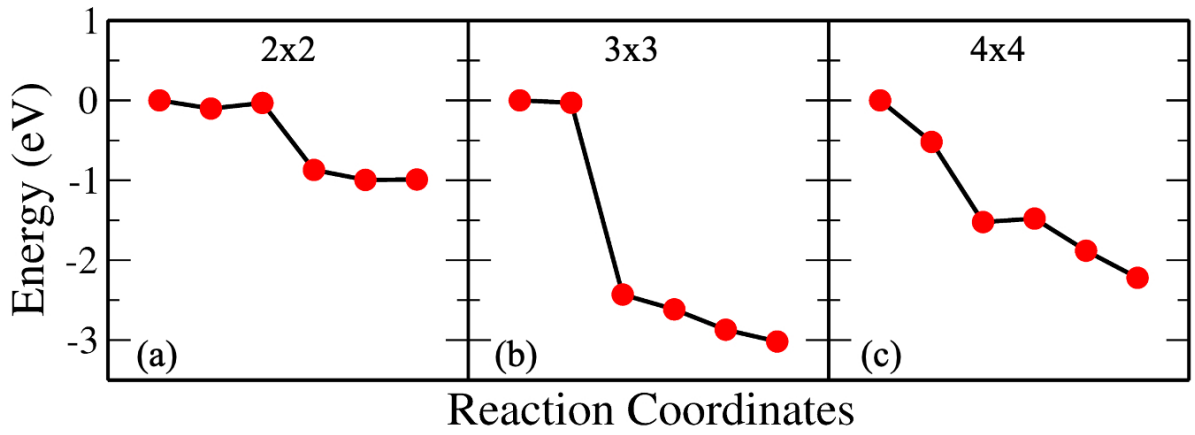

Fig. S11: (Color online) Heyrovsky reaction path for $H_{adsorbed}$ at P site on MoS_2/BP vdW HTSs for (a) 2×2, (b) 3×3 and(c) 4×4 supercell for 1/4 H^+ conc.

3×3 MoS_2/BP Configurations

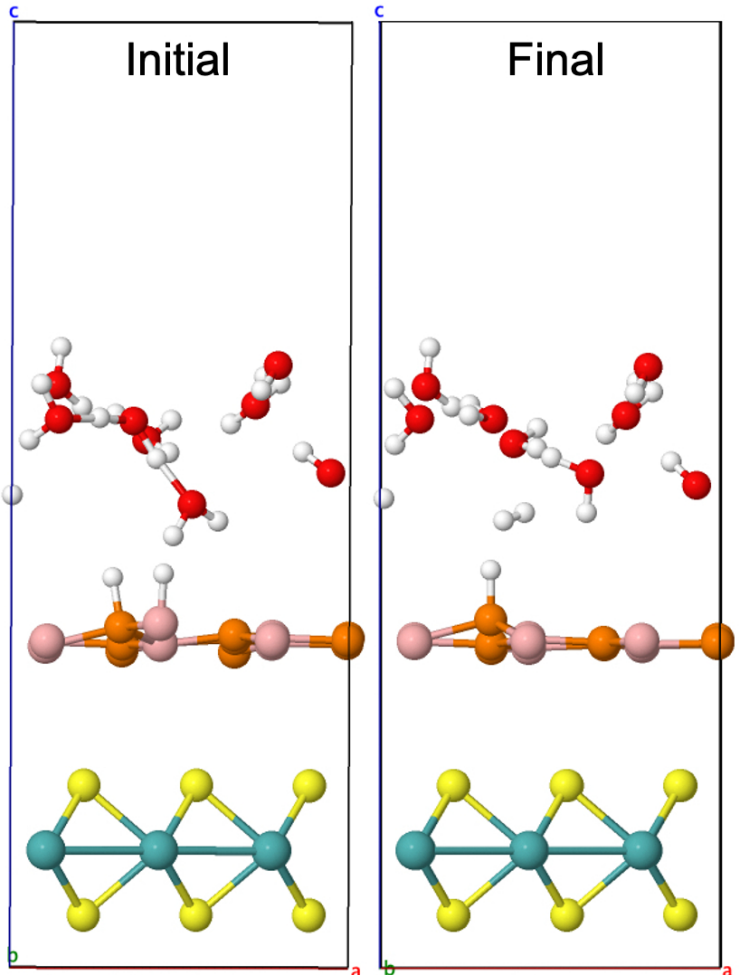

Fig. S12: (Color online) Initial and final configuration of 3×3 MoS_2/BP for Heyrovsky reaction.

3×3 MoS_2/BP Configurations With H_{down} Water Layer Orientation

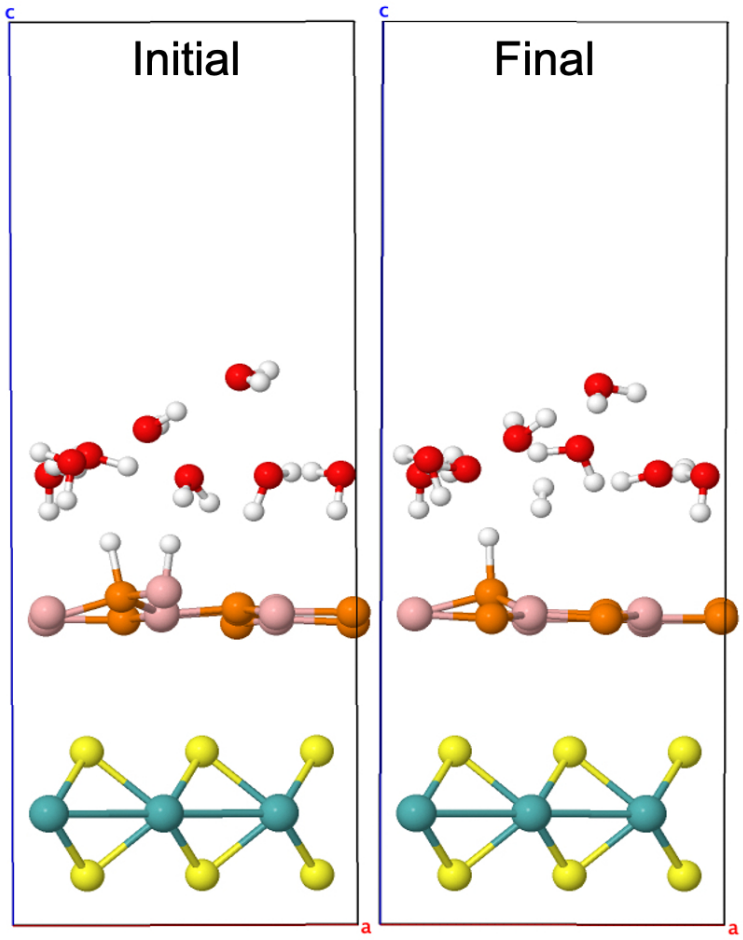

Fig. S13: (Color online) Initial and final configuration of 3×3 MoS_2/BP for Heyrovsky reaction in case H_{down} water layer orientation.

Electrode Potential of 2×2 MoS_2/BP and MoSSe/BP

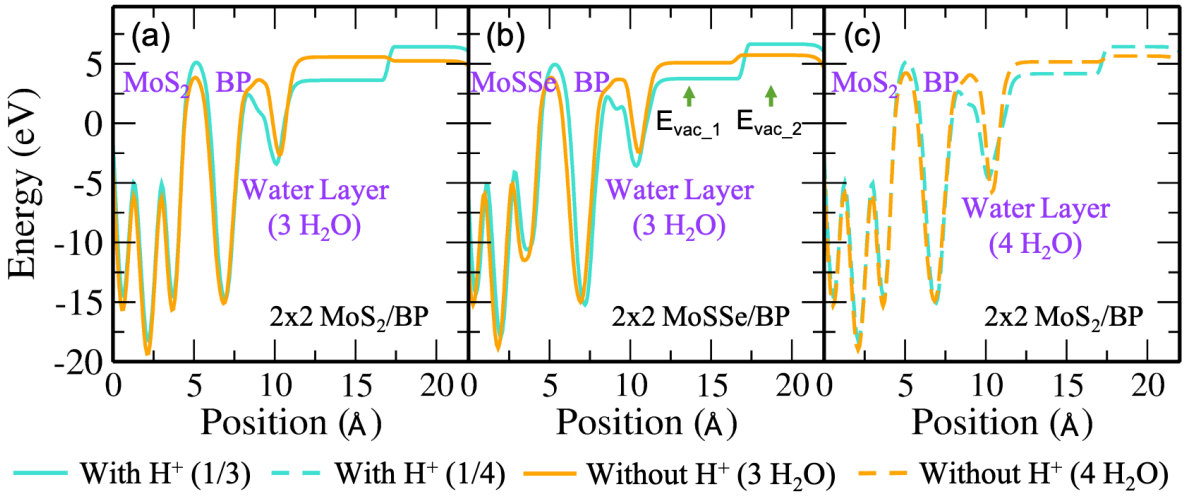

Fig. S14: (Color online) (a) Electrode potential for 2×2 MoS_2/BP with and without H^+ corresponding to 1/3 proton concentration and 3 H_2O, respectively. (b) Electrode potential for 2×2 MoSSe/BP with and without H^+ corresponding to 1/3 proton concentration and 3 H_2O, respectively. (c) Electrode potential for 2×2 MoS_2/BP with and without H^+ corresponding to 1/4 proton concentration and 4 H_2O, respectively.

Electrode Potential of 4×4 MoS_2/BP and MoSSe/BP

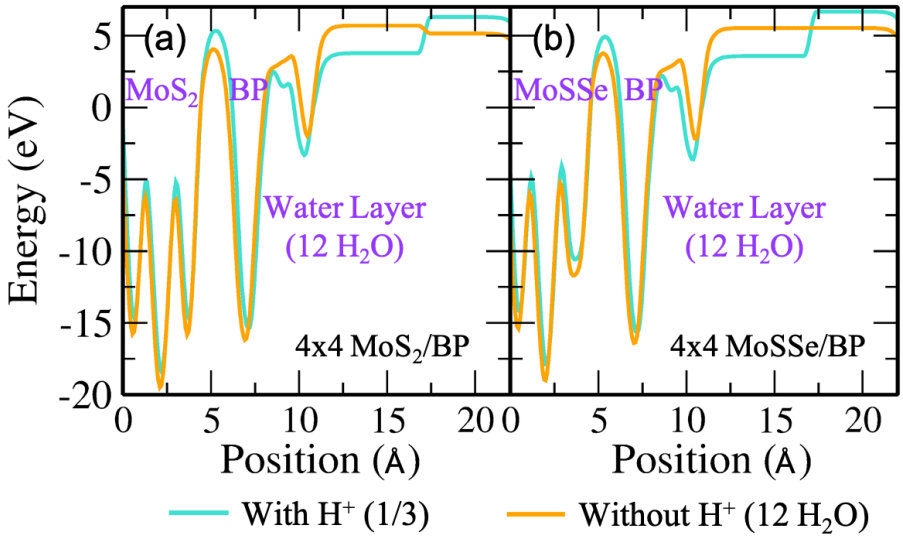

Fig. S15: (Color online) (a) Electrode potential for 4×4 MoS_2/BP with and without H^+ corresponding to 1/3 proton concentration and 12 H_2O, respectively. (b) Electrode potential for 4×4 MoSSe/BP with and without H^+ corresponding to 1/3 proton concentration and 12 H_2O, respectively.

H_{down} Water Orientation Reaction Path and Electrode Potential

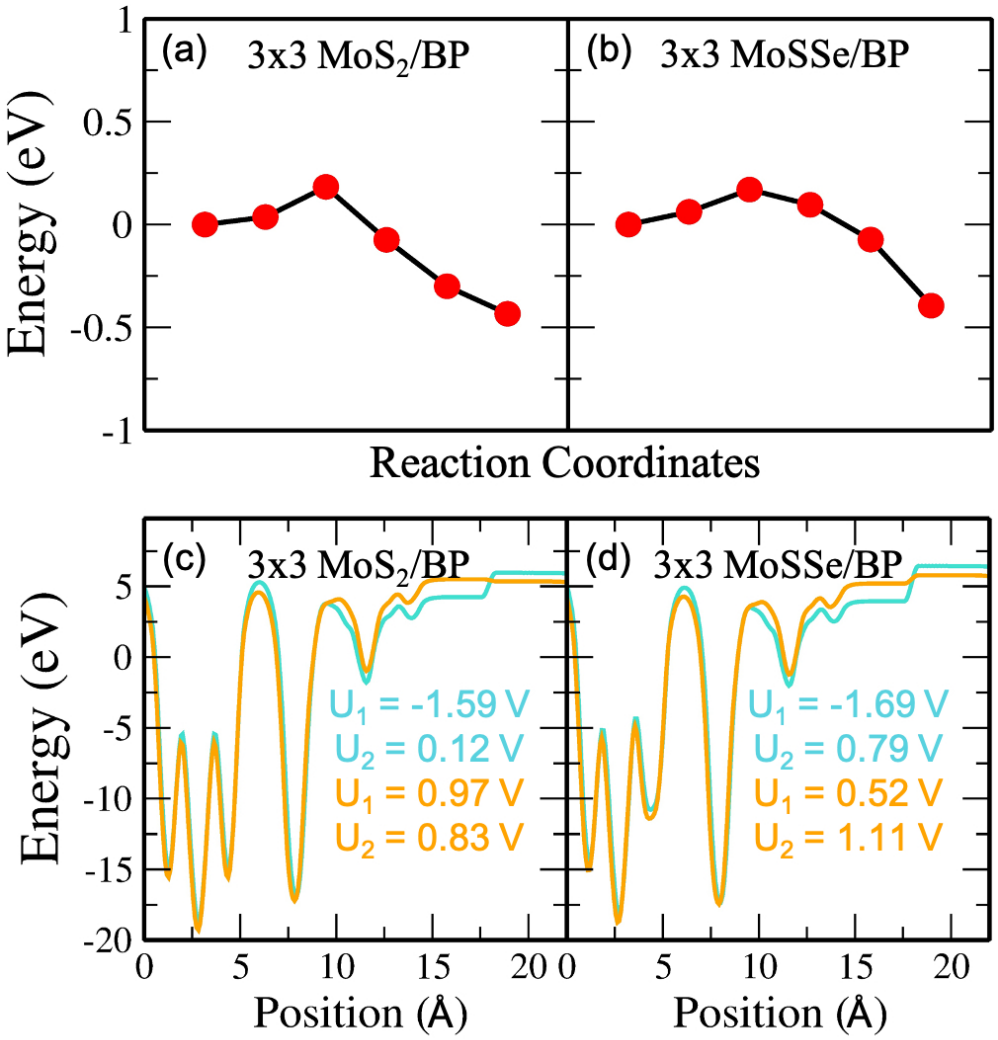

Fig. S16: (Color online) (a) and (b) Heyrovsky reaction step for MoS_2/BP and MoSSe/BP vdW HTS in 3×3 supercell with 1/8 proton concentration (c) and (d) Electrostatic potential plot of MoS_2/BP and MoSSe/BP vdW HTSs depicting water layer with and without H^+ in 3×3 supercell with 1/8 proton concentration and 8 water molecules, respectively.

Tafel Reaction Steps for 2×2 MoS_2/BP in case of $4H_2O$

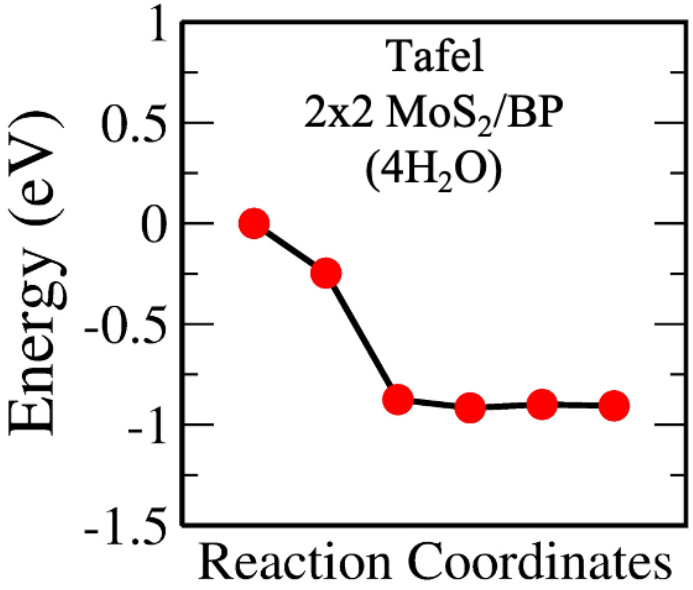

Fig. S17: (Color online) Tafel reaction step for 2×2 MoS_2/BP for 4 H_2O.